Photoinduced Immobilization of Biomolecules on the Surface of Azopolymer Films and Its Dependence on the Concentration and Type of the Azobenzene Moiety

Mamiko Narita, Fumihiko Hoshino, Makoto Mouri, Masaaki Tsuchimori, Taiji Ikawa, and Osamu Watanabe*

Toyota Central Research and Development Laboratories, Inc., Nagakute, Aichi, 480-1192, Japan

Received July 17, 2006; Revised Manuscript Received November 22, 2006

ABSTRACT: We report on the photoinduced immobilization of Immunoglobulin G (IgG) on the surface of azobenzene-bearing acrylate copolymers (azopolymers). Two different types of azopolymers were synthesized that incorporated either a 4-aminoazobenzene moiety (H-azopolymer) or a 4-aminocyanoazobenzene moiety (CN-azopolymer), using different concentrations of the respective moieties. IgG was immobilized on the surfaces of the azopolymer films by exposure to visible light, and each of the films was then treated with an aqueous solution of an antigen. Antigen−antibody reactions were confirmed on the surfaces of the films, indicating that immobilized IgG generated by a photoirradiation can retain its activity. The amount of the immobilized antibodies on the azopolymer surfaces increased with azobenzene content up to 30 wt % and saturated over 30 wt % when measured under the same conditions. The efficiency of the immobilization process was found to correlate with the depth of deformations on the surfaces of the azopolymers, which were characterized by comparison with deformations induced by polystyrene microspheres under the same conditions. The increased contact area produced by photodeformation could enhance the interactions between the antibodies and the azopolymer, thereby causing the antibodies to be more firmly immobilized. However, the photoimmobilization of IgG on H-azopolymers was superior to that on CN-azopolymers, even though their original hydrophilicities and adsorption efficiencies were almost the same. We confirmed that both the photoisomerization processes and retention rates of the immobilized antibodies were different for H- and CN-azopolymers. This suggests that the effectiveness of photoimmobilization is controlled not only by photodeformation but also by retention capability, which in turn depends on the chemical structure after photoirradiation.

Introduction

Biomolecules with specific molecular recognition capabilities have attracted much attention because of their potential for applications in biochips,[1,2] biosensors,[3,4] bioreactors,[5] and microactuators.[6] In order to take advantage of the functionality of these biomolecules, the provision of an immobilization process without deactivation is essential in order to obtain practical biomolecule carriers, especially for the creation of high-efficiency biosensors and biochips. Therefore, a number of immobilization techniques have been developed for biomolecules, in which the molecules are immobilized on a carrier using covalent bonds,[7,8] ionic bonds,[9] physical adsorption,[7,10] cross-linkage of the biomolecules,[11] or by microencapsulation.[12,13] Photoinitiated immobilization is one of the most powerful methods for the facile fabrication of immobilized patterns of biomolecules on a substrate.[14,15] However, photoirradiation sometimes triggers denaturation of proteins and damage to DNA due to the formation or cleavage of chemical bonds or by causing environmental changes.[16]

Polymers that contain azobenzene (azopolymers) are attractive materials because of their various photoresponses. Azobenzenes have been classified into three groups by spectroscopic analysis: azobenzene-type molecules, aminoazobenzene-type molecules, and pseudo-stilbene-type molecules.[17] The pseudo-stilbene-type molecules are characterized by the substitution of the 4- and 4′-positions of the two azobenzene rings with electron-donating and electron-withdrawing groups and hence are also described as "push−pull-type" azobenzenes. The surface of an azopolymer containing a push−pull-type azobenzene can be deformed under interference light irradiation to form a surface relief grating (SRG).[18−20] We found that polystyrene microspheres placed on an azopolymer can induce an indented structure after photoirradiation with visible light.[21−24] We have confirmed this deformation by using several types of microspheres with preselected diameters of between 2000 and 19 nm.[25,26] Diameters of less than 250 nm are beyond the diffraction limit, which indicates that deformation can also be induced by the near-field around microspheres that are small in diameter. A comparison between the indented structures and the calculated intensity distributions shows that the near-field around the microspheres does induce surface deformation.[27] We have applied this photoinduced deformation technique to a novel immobilization method for small objects.[28,29] Specifically, nanoscale macromolecules such as λ-deoxyribonucleic acid, immunoglobulin G (IgG), bacterial protease, and 1 μm diameter polystyrene particles have been immobilized on azopolymer surfaces by irradiation with visible light. Atomic force microscopy studies have revealed that biomolecules such as DNA and IgG can be immobilized by indent deformation to form an imprinted shape, in which the biomolecules are physically captured on the polymer surfaces without the formation of chemical bonds,[28] as shown in Figure 1.

This novel method is useful for the immobilization of a variety of small particles such as charged proteins, negatively charged DNA, and hydrophobic polystyrene microspheres on azopolymer surfaces, and it has been shown that the immobilized biomolecules can maintain their high-order structure without

* Corresponding author: e-mail e0909@mosk.tytlabs.co.jp; Tel +81-561-63-6169; Fax +81-561-63-6507.

10.1021/ma061601z CCC: $37.00
Published on Web 01/04/2007

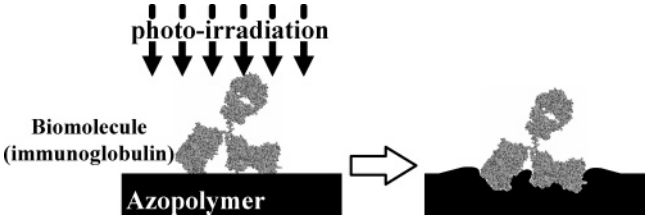

Figure 1. Schematic illustration of the photoimmobilization of a biomolecule (immunoglobulin) on the surface of an azopolymer. The surface of the azopolymer is deformed to the shape of the immunoglobulin after photoirradiation. The structure of the immunoglobulin was obtained from the Protein Data Bank.

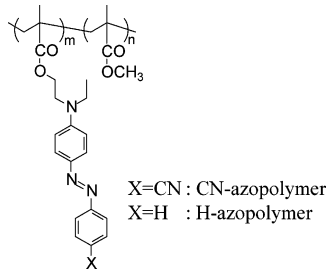

Figure 2. Structures of the azopolymers used in this research.

damage to their functionality. This versatility in terms of immobilization is a significant advantage of this technique. However, the mechanism for photoinduced immobilization on azopolymers and the dependence of immobilization efficiency on the chemical structure of the azobenzene moieties have not yet been examined in detail so far.

In this article, we compare the photoinduced immobilization of IgG on two types of azopolymers (shown in Figure 2) bearing various concentrations of 4-amino-4′-cyanoazobenzene (CN-azopolymer) or aminoazobenzene (H-azopolymer). CN-azopolymer and H-azopolymer contain a push−pull-type azobenzene and an aminoazobenzene, respectively. Photoinduced immobilization has been developed using azopolymers that include a push−pull-type azobenzene moiety; however, azopolymers bearing aminoazobenzene moieties have not been examined as yet. These azobenzenes have different adsorption spectra and should exhibit different deformation and immobilization features under photoirradiation. Therefore, we can obtain information about the photoimmobilization mechanisms by comparing these two types of azopolymers. First, we examined the relationship between immobilization efficiency and the indented depth with respect to the photoirradiation time and the specific azobenzene moiety. Second, we compared the relationship between immobilization efficiency and chemical structure and elucidated how this correlated with the photoisomerization properties and the retention rate of immobilized antibodies. We concluded that photoinduced immobilization was controlled not only by increasing the contact area between the IgG and the azopolymer surface but also by the capability of the IgG to be absorbed onto the azopolymer surface, and this could be changed by photoirradiation.

Experimental Section

Materials. Methyl methacrylate (MMA) purchased from Wako Pure Chemical Industries, Ltd., was used after first removing the inhibitor by flash column chromatography. Methacrylic acid and 2,2′-azobis(2-methylpropionitrile) (AIBN) from Tokyo Kasei Kogyo Co., Ltd., 4-dimethylaminopyridine from Wako Pure Chemical Industries, Ltd., water-soluble carbodiimide hydrochloride (WSCD·HCl) from Peptide Institute, Inc., phosphate-buffered saline (PBS) from Wako Pure Chemical Industries, Ltd., and Tween20 from Wako Pure Chemical Industries, Ltd., were used as-received without further purification. Cy5-linked Mouse IgG-to Goat IgG (Cy5-GIgG) from CHEMICON International, Inc., and Goat IgG to Rabbit IgG (H+L) (RIgG) from Bethyl Laboratories, Inc., were used as the biomolecules that were to be immobilized.

Table 1. Composition, Molecular Weight, and Glass Transition Temperature of the Azopolymers Used in This Study

polymer	azo-benzene	azo (mol %)[b]	azo (wt %)[b]	M_n[c]	M_w/M_n[c]	T_g (°C)[d]
CN-100	azo(CN)	100	100	[e]	[e]	124
CN-63		32	63	11 200	2.24	118
CN-39		15	39	18 500	1.89	121
CN-21		7	21	15 500	1.54	111
CN-5		1.5	5.0	17 400	1.43	111
H-100	azo(H)	100	100	15 900	2.62	100
H-63		34	63	7 100	2.60	101
H-29		11	29	10 500	1.89	102
H-5		1.5	4.9	17 800	1.41	117

[a] Polymerization conditions: 1 M monomers in DMF, AIBN 3 mol % for monomer, 60 °C for 3 h. [b] Estimated by ^{1}H NMR measurement. [c] Calculated by SEC (eluent: $CHC1_3$, PSt standards). [d] Determined from DSC measurements. [e] Not determined.

Azomonomer(CN) Synthesis. *N*-Ethyl-*N*-(2-hydroxyethyl)-4-(4-cyanophenylazo)aniline (azobenzene(CN)) was synthesized according to a previous report.[30] Azomonomer(CN) was synthesized as follows. A solution of methacrylic acid (2.04 g, 20.0 mmol) in dichloromethane (100 mL) was cooled to 0 °C, and WSCD·HCl (3.83 g, 20.0 mmol) was added slowly. Azobenzene(CN) (3.89 g, 13.2 mmol) in dichloromethane (100 mL) was added to this solution. 4-(Dimethylamino)pyridine (0.25 g, 2.05 mmol) was then added, and the solution was stirred for 12 h at ambient temperature. The solution was then washed twice with water, and the organic layer was dried over magnesium sulfate. After removing the solvent, the resulting material was purified by column chromatography (silica gel, ethyl acetate/hexane = 1/3) followed by recrystallization (ethyl acetate/hexane = 1/3). Yield: 4.14 g (87%). ^{1}H NMR ($CDCl_3$, δ in ppm): 7.88 (m, 4H, CH in aromatic), 7.76 (m, 2H, CH in aromatic), 6.81 (d, 2H, CH in aromatic), 6.11 (s, 1H, CH in double bond), 5.60 (t, 1H, CH in double bond), 4.37 (t, 2H, $-NCH_2CH_2O-$), 3.73 (t, 2H, $-NCH_2CH_2O-$), 3.54 (q, 2H, $-NCH_2CH_3$), 1.94 (s, 3H, $=C-CH_3$), 1.26 (t, 3H, $-NCH_2CH_3$).

Azomonomer(H) Synthesis. *N*-Ethyl-*N*-(2-hydroxyethyl)-4-(phenylazo)aniline (azobenzene(H)) was synthesized according to a previous report.[30] Azomonomer(H) was also synthesized using the above procedure for azomonomer(CN). The product was purified by column chromatography (silica gel, ethyl acetate/hexane = 1/10 v/v as eluent). ^{1}H NMR ($CDCl_3$, δ in ppm): 7.86 (m, 4H, CH in aromatic), 7.47 (t, 2H, CH in aromatic), 7.37 (t, 1H, CH in aromatic), 6.80 (d, 2H, CH in aromatic), 6.11 (s, 1H, CH in double bond), 5.58 (t, 1H, CH in double bond), 4.35 (t, 2H, $-NCH_2CH_2O-$), 3.69 (t, 2H, $-NCH_2CH_2O-$), 3.50 (q, 2H, $-NCH_2CH_3$), 1.94 (s, 3H, $=C-CH_3$), 1.23 (t, 3H, $-NCH_2CH_3$).

Polymerization Procedure. The procedure for CN39 is described as a typical example in Table 1. A solution of azomonomer(CN) (545 mg, 1.5 mmol) and methyl methacrylate (932 mg, 9.3 mmol) in DMF (10mmol) was substituted into a nitrogen atmosphere by bubbling with nitrogen. After the addition of AIBN (51.5 mg, 0.31 mmol), polymerization was performed for 3 h at 60 °C. The solution was added slowly to methanol to precipitate the polymer. The azopolymer was obtained by filtration followed by drying in vacuo at 60 °C for 24 h. Yield: 928 mg (63%). The average molecular weight of the polymer was measured by size exclusion chromatography (SEC, eluent $CHCl_3$, Shodex. GPC-101 with K-805L, Showa Denko KK) calibrated with standard polystyrene. The copolymerization ratio was calculated on the basis of the integration ratio of ^{1}H NMR measurements. The glass transition temperature (T_g) was determined by differential scanning calorimetry (DSC, TA Instruments Q1000, heating rate, 10 °C/min). The characterization data are summarized in Table 1. All of the azopolymers had almost the same molecular weights and high glass transition temperatures of between 100 and 124 °C.

Azopolymer Film Preparation. Azopolymer films were prepared as follows. An azopolymer−pyridine solution (12.5 g/L) was spin-coated onto a glass slide after filtration through a Teflon membrane filter (Millipore, 0.22 μm). The films were placed in a vacuum oven at 60 °C for 2 h to obtain solvent-free samples. The films that we used were 40 nm thick, as determined by absorbance measurements at the wavelength of maximum absorption. The absorbance of the azopolymer films was measured using a spectrophotometer (Shimadzu Corp., UV-2100). The values of λ_{max} for the CN- and H-azopolymer films were 450 and 410 nm, respectively.

Photodeformation of the Azopolymer Films. We analyzed the deformation properties of the azopolymers by using microspheres.[21−27] An aqueous solution including polystyrene microspheres (Duke Scientific Corp., diameter 250 nm) was dropped onto the surfaces of the polymer films, and then the spheres were allowed to arrange themselves by a self-organization process. After drying the samples at room temperature, they were irradiated using an LED array-irradiation apparatus (peak emission wavelength: 470 nm; power density: 20 mW/cm^2). The polymer films were washed in an ultrasonic bath in order to remove excess PS spheres from the surfaces of the azopolymer. After drying the polymer surfaces, they were investigated using atomic force microscopy (AFM, Nanoscope E Digital Instruments Inc.) under ambient conditions, and the depths of the indents that were formed were determined.

Immobilization Efficiency for IgG and the Activity of the Immobilized IgG. In order to verify the immobilization properties of the films, Cy5-GIgG was selected as a suitable protein to be immobilized. In order to verify the activity of this immobilized IgG, RIgG was used as an immobilization antibody and Cy5-GIgG was used as an antigen to RIgG. Cy5-GIgG and RIgG were diluted to 500−10 ng/mL in phosphate-buffered saline solutions (PBS) with 0.01% v/v Tween20. PBS solutions of Cy5-GIgG and RIgG were spotted at different concentrations on the surfaces of the azopolymers. The spotted films were dried in vacuo and were then irradiated with blue visible light for 30 min using an LED array. After washing in PBS solution to remove excess unimmobilized antibodies, immune reactions were performed for 30 min by reacting with a 1% Cy5-GIgG gelatin solution. After washing followed by drying, the fluorescence intensities emitted from the spots on the polymer surfaces were measured using a microarray scanner (Affymetrix 428 Array Scanner, Affymetrix Japan K.K.). The immobilization performance was determined by analyzing the fluorescence intensity of the immobilized Cy5-GIgG and the activity for Cy5-GIgG captured by RIgG.

Contact Angle Measurements. Contact angle measurements were performed using a Drop-master 500 (Kyowa Interface Science Co., Ltd., Japan). Ion-exchanged water droplets of 2 μL in volume were dropped onto the azopolymer films, and then the contact angles were measured by the half-angle measuring method 1 s after the spotting process.

Retention Capability for Immobilized Antibodies. The retention capabilities of the various films for immobilized antibodies were determined by measuring the amounts of antibodies remaining on the azopolymers after washing in PBS. After treatment for a given number of hours and subsequent drying, the intensity of the photoluminescence obtained from the immobilized Cy5-GIgG was measured using a microarray scanner. The treatment process was repeated after every measurement. The azopolymer films were measured using a microarray scanner after 6, 20, and 28 h of stirring.

Dynamics of Isomerization and Reorientation. The photoinduced dynamics of the azobenzene moieties in the films were estimated in accordance with the method described by Blanche et al.[31] Changes in the optical densities of the films with time were measured using linearly polarized probe light during and after irradiation with a linearly polarized pump light. Two different polarized probe lights at 0° and 90° from the polarization direction of the pump light were used to analyze the dynamics of the azobenzene moieties. The back-isomerization process (from cis-to-trans) that occurs after turning off the light was estimated from the averaged optical density, and the degree of photoinduced reorientation was estimated from the relative anisotropy.

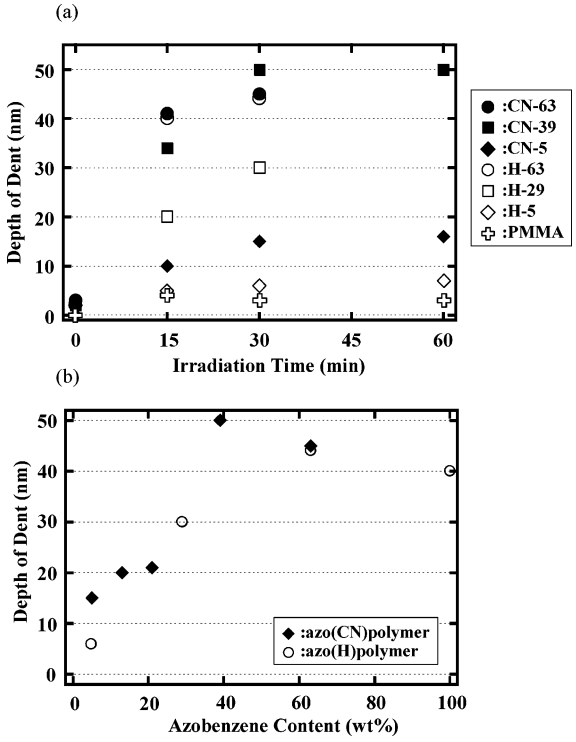

Figure 3. (a) Changes in dent depth as a function of photoirradiation time for CN-azopolymers (solid figures) and H-azopolymers (open figures). The numbers show the weight content of the azo moieties. The open crosses show the control experiment using PMMA. (b) Changes in the dent depth as a function of azobenzene content. The results were obtained after 30 min of photoirradiation.

Results and Discussion

The photodeformation capabilities of the CN-azopolymer and the H-azopolymer were examined by determining the depth of indents formed by polystyrene microspheres under LED irradiation. After photoirradiation and removal of the microspheres, regularly arranged indented patterns formed by the microspheres were observed on the surfaces of the azopolymers. The depths of the indents were plotted as a function of irradiation time for several kinds of azopolymers, as shown in Figure 3a. No noticeable features were observed after the process was performed without irradiation for any of the azopolymers. A film of poly(methyl methacrylate) (PMMA, M_n = 20 500, MWD = 1.33) was used as a control sample; this contains no photoresponsive molecules, and the surface of the PMMA was not changed after photoirradiation. The indent depths in the azopolymer increased with increasing irradiation time. The depths of the indents saturated and reached a maximum after 30 min of photoirradiation for each of the azopolymers. The saturated depths were lowest in the azopolymers with the lowest content of azobenzene moieties. These results indicate that the photoresponsive moiety plays an important role in inducing photodeformation and that the indent depth is related to the content of the azobenzene in the azopolymers. Some azopolymers immobilized the polystyrene microspheres too firmly for them to be removed from the surface of the azopolymers after 60 min of photoirradiation, and thus their depths could not be measured.

The indent depths were almost saturated after 30 min of photoirradiation for all of the azopolymers that were examined, and thus this irradiation time was fixed in our later experiments.

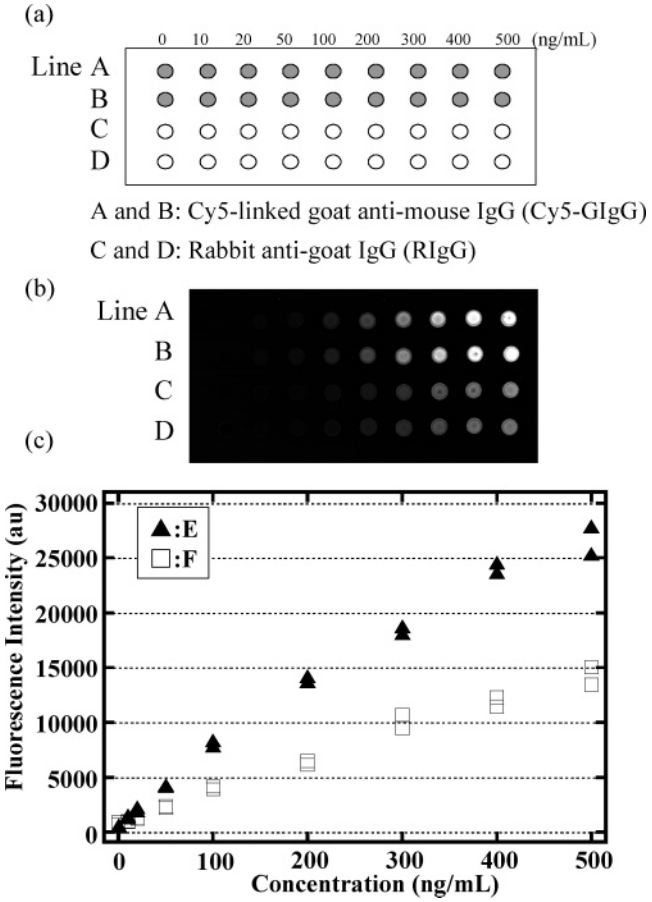

Figure 4. (a) Spotting layout of antibodies on azopolymer films for measuring the efficiency of the immobilization of IgG and the activity of immobilized IgG. The spots were all arrayed on the azopolymer film at the same time. (b) Fluorescence image of the above slide after the immobilization process measured using an array scanner. Lines A and B represent Cy5-GIgG; lines C and D represent RIgG reacted with Cy5-GIgG. (c) Measured fluorescence intensities of the spotted region as a function of concentration. Line E (solid triangles) is based on lines A and B, and line F (open squares) is based on lines C and D in (b).

Figure 3b shows the relationship between the depth of the dents after 30 min of photoirradiation and the azobenzene content. The indent depth increased with the relative content of azobenzene moiety and saturated at over 30 wt % of azobenzene content. There was no difference in photodeformation capability between the CN- and H-azopolymers, even though they contained different types of azobenzene. The results show that H-azopolymers could exhibit immobilization capabilities similar to CN-azopolymers, despite the differences of chemical structure. These azopolymers were then applied for the photoimmobilization experiments.

Photoimmobilization of IgGs was performed by photoirradiation for 30 min in order to examine the efficiency of the immobilization process. The spotting layout is shown in Figure 4a, and a typical scanning image is shown in Figure 4b, in which the intensities of the spots on lines A and B show the amount of immobilized Cy5-GIgG and those on lines C and D show the amount of Cy5-GIgG captured by the immobilized RIgG. The observation of fluorescence on lines A and B shows that antibodies were immobilized on the azopolymer films, while lines C and D indicate that the photoimmobilized antibodies retain their immunoreactivity after the photoirradiation process. The fluorescence intensities of all the spots were plotted as a function of the concentrations of the spot solutions, and it was found that the intensities increased linearly with concentration. The IgGs could be immobilized evenly over the surface in this concentration range. The data are shown plotted linearly in lines E and F of Figure 4c. The entire surfaces of the azopolymer films were treated with an aqueous solution containing Cy5-GIgG in order to perform the immune reactions. The intensity of the fluorescence did not increase after the immune reactions, other than at the spots where the RIgG was immobilized. This means there was no influence on the adsorption by postprocessing after the photoimmobilization process and that the fluorescence of the immobilized Cy5-GIgG could be observed correctly as a result of the first immobilization process. Line E (solid triangles) is based on lines A and B, while line F (open squares) is based on lines C and D in Figure 4a. We consider that the slope of line E is an index of the efficiency for the immobilization of antibodies, and the slope of line F is an index of the activity of the immobilized antibodies. The ratio of these slopes (E/F) represents the ratio of the active sites to the immobilized antibodies, which could be related to the degree of orientation of the immobilized antibodies. The azopolymer showed some intrinsic fluorescence under observation by the array scanner, but the intensity was negligible in this experiment.

We employed the relative value for the slope efficiency of the photoimmobilization to avoid fluctuations in the absolute values originating from the relative humidity of the drying conditions, and we always used the CN39 azopolymer as a standard. The relative efficiency of the photoimmobilization on each azopolymer was calculated from the gradient of the slope compared to the CN39 azopolymer. The relative efficiencies of the photoimmobilization on the azopolymers were plotted as a function of the azobenzene content, as shown in Figure 5a. The immobilization efficiencies of both the CN- and H-azopolymers increased with azobenzene content up to about 30 wt % and then became saturated at ca. 30 wt % of azobenzene content, although the saturated values were different between the CN- and H-azopolymers. On the other hand, the photoinduced immobilization of Cy5-GIgG using PMMA as an immobilization substrate showed very low immobilization efficiency (less than 10%) when compared with the CN-39 azopolymer. This result indicates that an azobenzene moiety that exhibits photoisomerization is essential in order to immobilize IgGs on azopolymers by using a photoimmobilization process.

The activities were determined from the photoluminescence intensities of the Cy5-GIgG captured by the photoimmobilized RIgG. The ratio of the slope compared to the CN-39 azopolymer was also defined as the relative activity of the photoimmobilized IgG on each azopolymer. The relative activity of the photoimmobilized IgG on the azopolymers was then plotted as a function of the azobenzene content, as shown in Figure 5b. The relative activity of the photoimmobilized RIgG on the azopolymers increased with increasing azobenzene content up to 30 wt % and then saturated over 30 wt %, which is the same relationship as that of the relative efficiency of the immobilization of Cy5-GIgG. The relationship between the immobilization efficiency and the activity of the immobilized IgG provides useful information concerning the orientation of the immobilized IgG. We compared relative efficiency with the activity in all of the experiments and found that the relationships were almost the same for all of the azopolymers, irrespective of the content and chemical structures of their azo moieties. In this article, we concluded that the degree of orientation of the immobilized IgG on all of the azopolymers was almost the same, while the efficiency of the immobilization was affected by the content and the chemical structures of the azo moieties.

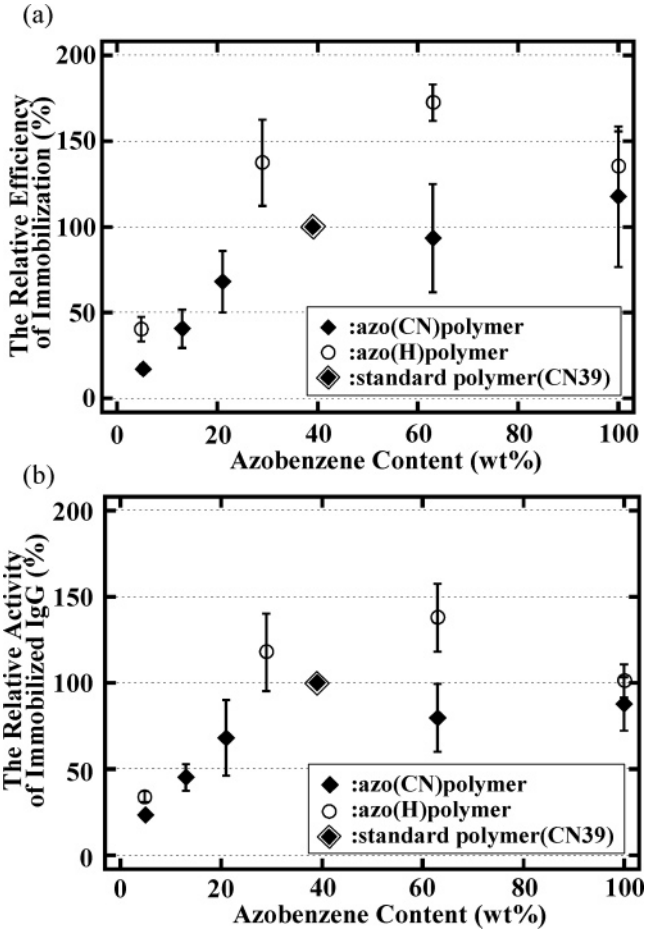

Figure 5. (a) Dependence of the relative immobilization efficiency of Cy5-IgG on azopolymer content. The solid diamonds and open circles represent CN- and H-azopolymers, respectively. CN-39 was used as the standard polymer, as shown by the solid diamond in an open diamond.

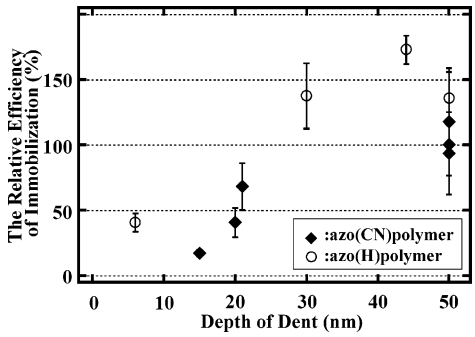

Figure 6. Relationship between the dent depth and the relative immobilization efficiency of Cy5-GIgG. The solid diamonds and the open circles represent CN- and H-azopolymers, respectively.

The dependences of the indent depth and the immobilization efficiency for IgGs on the azo content of the films exhibit similar tendencies for both azopolymers. Next, we confirmed the relationship between the immobilization of IgG and the deformation efficiency of the azopolymer. The relative immobilization efficiencies were plotted as a function of indent depth, as shown in Figure 6. Incremental changes in the immobilization efficiency were observed by increasing in the depth of the dents. These results demonstrate that increasing the contact area between the azopolymer surface and the IgGs brings about improved immobilization of the IgGs. On the other hand, the immobilization efficiency of the H-azopolymers was higher than that of the CN-azopolymers across the whole range, and this is also shown in Figure 5a. This difference shows that the degree of photoimmobilization not only is affected by the deformation capability but also is a property of the surface of the azopolymer and is related to the chemical structure of the azobenzene incorporated in the azopolymer. Whitesides et al. have also reported that immobilization is influenced by the properties of the surface.[32−34] The content and chemical structure of the azobenzene could contribute to the different features that are observed for the different surfaces of these azopolymers.

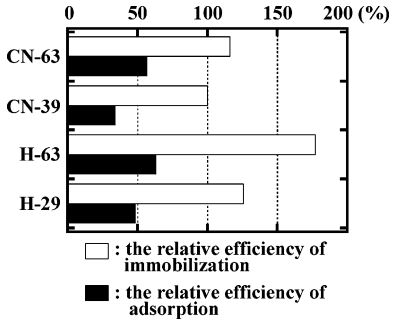

Figure 7. Adsorption properties of Cy5-GIgG on the azopolymers.

The contact angle of water on the azopolymer surfaces was measured to compare their surface hydrophilicities because the adsorption capability of the polymer surface for biomolecules could be influenced by the nature of the surface in terms of hydrophilicity or hydrophobicity. The measured contact angles were almost the same ($72 \pm 3°$) for every azopolymer and for PMMA. All of the azopolymers in this experiment showed a hydrophobic surface, irrespective of the structure and content of the azobenzenes. The surface hydrophobicity of the azopolymers meant that there were no clear differences in the immobilization efficiency for IgG on each azopolymer. Although the surface hydrophobicities of each of the azopolymers were similar, interactions between antibodies and the surface of the azopolymers could be different for each of the films that we tested. Therefore, we tried to examine the efficiency of the adsorption of antibodies onto the surfaces of the azopolymers. The adsorption efficiency for antibodies was determined by the efficiency of the immobilization without photoirradiation. The ratio of the slope with respect to that of the CN-39 azopolymer was used as the relative efficiency for the adsorption of antibodies. The relative adsorption efficiency of Cy5-GIgG on the azopolymers is shown in Figure 7. The relative adsorption efficiency was lower than the relative photoimmobilization efficiency, which also demonstrates that photoirradiation is an important process to firmly immobilize most of the antibodies. The relationship between the relative adsorption efficiency and the relative immobilization efficiency of Cy5-GIgG on each of the azopolymers was almost the same. Although the adsorption efficiency of the H-azopolymer was slightly higher than that of the CN-azopolymer, the difference was not sufficient to explain the differences in the immobilization efficiencies.

We thought that the adsorption properties of the azopolymers may have been equal originally and that the differences in the photoimmobilization efficiencies could be generated from the photoirradiation process. Changes in adsorption efficiency after photoirradiation could have occurred through photoirradiation or photoinduced reorientation processes in the azopolymer system. As described above, H-azopolymer and CN-azopolymer are classified as different polymer categories, and they undergo different photoprocesses. In order to characterize these photoprocesses, the adsorption capabilities of the azopolymers after photoirradiation should be considered. We used the retention rate of photoimmobilized antibodies after the washing process

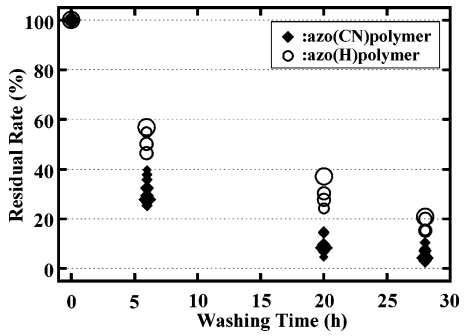

Figure 8. Retention capability of immobilized Cy5-GIgG of the azopolymers. The solid diamonds and the open circles represent CN- and H-azopolymers, respectively. The sizes of the solid diamonds and the open circles represent the concentration of azobenzene. The largest represent CN-100 and H-100, and the smallest represent CN-21 and H-29, respectively.

to define the adsorption capability after photoirradiation. The method used to obtain photoimmobilization included a washing process, and the immobilization efficiency was obtained after washing. Therefore, the immobilization efficiency could be affected by the retention capability for immobilized antibodies on the surfaces of the azopolymers during washing. We measured the amount of residual immobilized antibodies to elucidate the retention capability for antibodies on each azopolymer. Azopolymer films carrying Cy5-GIgG that had been immobilized by photoirradiation were held in stirred PBS in order to remove the antibodies from the surfaces of the azobenzene films. The amount of residual immobilized Cy5-GIgG was estimated by measuring the fluorescence intensity after 6, 20, and 28 h of stirring; the results were then plotted, as shown in Figure 8. All of the H-azopolymers exhibited much better retention rates than the equivalent CN-azopolymers. These results indicate that the adsorption efficiency of antibodies on the H-azopolymers after photoirradiation changed more than it did on the CN-azopolymers, such that the amount of the immobilized antibodies remaining on the H-azopolymer films was more than that on the CN-azopolymer films after the washing process. Therefore, the H-azopolymers could procure a higher affinity or adsorptive capability for antibodies after the photoirradiation process. The size of each mark in Figure 8 represents the azobenzene concentration; the largest marks are for CN-100 and H-100, while the smallest ones are for CN-21 and H-29, respectively. The residual rate showed no correlation with the azobenzene content for both H- and CN-azopolymers that included sufficient azobenzene moieties.

There are several factors that induce changes in the adsorption capability after photoirradiation. There are remarkable differences between the CN- and H-azopolymers in terms of the photoisomerization phenomena that occur on the azobenzene moieties. CN-azopolymer includes a push−pull-type azobenzene that has electron-donating and electron-withdrawing groups at the ends of the azobenzene, while H-azopolymer contains an amino-type azobenzene that only has an amino group. It has been reported that H-azopolymer (aminoazobenzene) shows a relatively stable cis state after trans−cis isomerization by photoirradiation.[17,20] We also confirmed a stable cis state in the film of H-azopolymer by measuring the changes with time of the absorption capability of the films using a probe light during and after photoirradiation. In the case of the CN-azopolymer films, the cis state was almost totally back-isomerized 30 min after the light was turned off. On the other hand, the H-azopolymer films showed a stable cis state, and the relaxation time of the cis state was over 160 h, which was the time calculated from the recovery curve of the absorbance of the trans state. The stable cis state of the H-azopolymer could be an important factor that influences changes in its adsorption capability after photoirradiation. Reorientation of the azobenzene moieties, as estimated from the relative anisotropy, was certainly induced in the films of both azopolymers. However, the relaxation occurred quickly, within 5−8 min. The effect of reorientation on the immobilization efficiency could be minimal in this experiment. We also determined the contact angle after photoirradiation; however, the values did not change after the photoirradiation for every azopolymer. Although hydrophobicity did not change during photoirradiation, a stable cis isomer in the case of the H-azopolymer would provide favorable conditions for the immobilization of antibodies. The reason why the stable cis state enhances the adsorption capability is still unclear. Changes in the dipole moment or in the basicity due to the photoirradiation should be taken into consideration.

Conclusion

A novel method for the photoimmobilization of biomolecules onto azopolymers has been discussed. We can now confirm the photoimmobilization capabilities of CN-azopolymers and H-azopolymers, though these are different categories of polymer. IgG could be firmly immobilized on the surfaces of the azopolymers after photoirradiation, and the activity of IgG was maintained after the photoimmobilization, which indicated that the immobilized IgG on the azopolymers preserved its higher-order structure after the immobilization process. Under the same conditions, the amount of immobilized IgG on the azopolymer surfaces increased with increasing azobenzene content up to 30 wt % and saturated over 30 wt %. The immobilization efficiency for IgG basically correlated with the deformation depth of the surface of the azopolymers, which was characterized relative to the depth of indents formed by polystyrene microspheres under the same conditions. Increasing the contact area by photodeformation could enhance interactions between the antibodies and the azopolymers such that the antibodies are immobilized more strongly. On the other hand, we found that the immobilization efficiency of antibodies on H-azopolymers is higher than it is on CN-azopolymers. We confirmed that the original adsorption efficiency of H-azopolymers was almost the same as that of CN-azopolymers. However, the retention capability and the isomerization properties of CN- and H-azopolymers were different. We concluded that the photoimmobilization capability is controlled not only by photodeformation but also by the retention capability, depending on the chemical structure after photoirradiation.

Supporting Information Available: Experimental results of stability of azopolymer under treating in water solution and dynamics of isomerization and reorientation of azo moiety. This material is available free of charge via the Internet at http://pubs.acs.org.

References and Notes

(1) *Protein Microarray Technology*; Kambhampati, D., Ed.; Wiley-VCH: Weinheim, 2003.
(2) *Protein Microarrays*; Schena, M., Ed.; Jones and Bartlett Publishers: Sudbury, 2004.
(3) Schuck, P. *Annu. Rev. Biophys. Biomol. Struct.* **1997**, *26*, 541.
(4) Cosnier, S. *Biosens. Bioelectron.* **1999**, *14*, 443.
(5) Guzman, N. A.; Park, S. S.; Schaufelberger, D.; Hernandez, L.; Paez, X.; Rada, P.; Tomlinson, A. J.; Naylor, S. *J. Chromatogr., B* **1997**, *697*, 37.
(6) Nicolini, C. *Biosens. Bioelectron.* **1995**, *10*, 105.
(7) Wilson, D. S.; Nock, S. *Curr. Opin. Chem. Biol.* **2001**, *6*, 81.

(8) Feng, C. L.; Zhang, Z.; Forch, R.; Knoll, W.; Vancso, G. J.; Schonherr, H. *Biomacromolecules* **2005**, *6*, 3243.
(9) Lee, Y.; Lee, E. K.; Cho, Y. W.; Matsui, T.; Kang, I.-C.; Kim, T.-S.; Han, M. H. *Proteomics* **2003**, *3*, 2289.
(10) Ouyang, Z.; Takats, Z.; Blake, T. A.; Gologan, B.; Guymon, A. J.; Wiseman, J. M.; Oliver, J. C.; Davisson, V. J.; Cooks, R. G. *Science* **2003**, *301*, 1351.
(11) Levy, I.; Shoseyov, O. *Curr. Protein Pept. Sci.* **2004**, *5*, 33.
(12) Gill, I.; Ballesteros, A. *Trends Biotechnol.* **2000**, *18*, 282.
(13) Hartmann, M. *Chem. Mater.* **2005**, *17*, 4577.
(14) Yang, Z.; Frey, W.; Oliver, T.; Chilkoti, A. *Langmuir* **2000**, *16*, 1751.
(15) Christman, K. L.; Maynard, H. D. *Langmuir* **2005**, *21*, 8389.
(16) Ostuni, E.; Chapman, R. G.; Holmlin, R. E.; Takayama, S.; Whitesides, G. M. *Langmuir* **2001**, *17*, 5605.
(17) Rabek, J. F. *Photochemistry and Photophysics 2*; CRC Press: Boca Raton, FL, 1990; Chapter 4.
(18) Delaire, J. A.; Nakatani, K. *Chem. Rev.* **2000**, *100*, 1817.
(19) Natansohn, A.; Rochon, P. *Chem. Rev.* **2002**, *102*, 4139.
(20) Karageorgiev, P.; Neher, D.; Schulz, B.; Stiller, B.; Pietsch, U.; Giersig, M.; Brehmer, L. *Nat. Mater.* **2005**, *4*, 699.
(21) Kawata, Y.; Egami, C.; Nakamura, O.; Sugihara, O.; Okamoto, N.; Tsuchimori, M.; Watanabe, O. *Opt. Commun.* **1999**, *161*, 6.
(22) Hasegawa, M.; Ikawa, T.; Tsuchimori, M.; Watanabe, O.; Kawata, Y. *Macromolecules* **2001**, *34*, 7471.
(23) Watanabe, O.; Ikawa, T.; Hasegawa, M.; Tsuchimori, M.; Kawata, Y. *Appl. Phys. Lett.* **2001**, *79*, 1366.
(24) Watanabe, O.; Ikawa, T.; Narita, M.; Tsuchimori, M. *J. Photopolym. Sci. Technol.* **2004**, *17*, 403.
(25) Watanabe, O.; Ikawa, T.; Hasegawa, M.; Tsuchimori, M.; Kawata, Y.; Egami, C.; Sugihara, O. *Mol. Cryst. Liq. Cryst. Sci. Technol., Sect. A* **2000**, *345*, 305.
(26) Ikawa, T.; Mitsuoka, T.; Hasegawa, M.; Tsuchimori, M.; Watanabe, O.; Kawata, Y. *J. Phys. Chem. B* **2000**, *104*, 9500.
(27) Ikawa, T.; Mitsuoka, T.; Hasegawa, M.; Tsuchimori, M.; Watanabe, O.; Kawata, Y. *Phys. Rev. B* **2001**, *64*, 195408.
(28) Ikawa, T.; Hoshino, F.; Matsuyama, T.; Takahashi, H.; Watanabe, O. *Langmuir* **2006**, *22*, 2747.
(29) Watanabe, O.; Ikawa, T.; Kato, K.; Tawada, M.; Shimoyama, H. *Appl. Phys. Lett.* **2006**, *88*, 2040107.
(30) Ho, M. S.; Natansohn, A.; Barrett, C.; Rochon, P. *Can. J. Chem.* **1995**, *73*, 1773.
(31) Blanche, P.-A.; Lemaire, Ph. C.; Dumont, M.; Fischer, M. *Opt. Lett.* **1999**, *24*, 1349.
(32) Prime, K. L.; Whitesides, G. M. *J. Am. Chem. Soc.* **1993**, *115*, 10714.
(33) Sigal, G. B.; Mrksich, M.; Whitesides, G. M. *J. Am. Chem. Soc.* **1998**, *120*, 3464.
(34) Ostuni, E.; Chapman, R. G.; Holmlin, R. E.; Takayama, S.; Whitesides, G. M. *Langmuir* **2001**, *17*, 5605.

MA061601Z